

## New rubrolide analogues as inhibitors of photosynthesis light reactions



Jodieh O.S. Varejão<sup>a</sup>, Luiz C.A. Barbosa<sup>a,b,\*</sup>, Gabriela Álvarez Ramos<sup>c</sup>, Eduardo V.V. Varejão<sup>a</sup>, Beatriz King-Díaz<sup>c</sup>, Blas Lotina-Hennsen<sup>c</sup>

<sup>a</sup> Department of Chemistry, Universidade Federal de Viçosa, Av. P.H. Rolfs, s/n, 36570-000 Viçosa, MG, Brazil

<sup>b</sup> Department of Chemistry, Universidade Federal de Minas Gerais, Av. Pres. Antônio Carlos, 6627, Campus Pampulha, CEP 31270-901 Belo Horizonte, MG, Brazil

<sup>c</sup> Department of Biochemistry, School of Chemistry, National Autonomous University of México, México, D.F. C.P. 04510, Mexico

### ARTICLE INFO

#### Article history:

Received 4 December 2014

Received in revised form 9 February 2015

Accepted 19 February 2015

Available online 26 February 2015

### ABSTRACT

Natural products called rubrolides have been investigated as a model for the development of new herbicides that act on the photosynthesis apparatus. This study comprises a comprehensive analysis of the photosynthesis inhibitory ability of 27 new structurally diverse rubrolide analogues. In general, the results revealed that the compounds exhibited efficient inhibition of the photosynthetic process, but in some cases low water solubility may be a limiting factor. To elucidate their mode of action, the effects of the compounds on PSII and PSI, as well as their partial reaction on chloroplasts and the chlorophyll *a* fluorescence transients were measured. Our results showed that some of the most active rubrolide analogues act as a Hill reaction inhibitors at the  $Q_B$  level by interacting with the  $D_1$  protein at the reducing side of PSII. All of the active analogues follow Tice's rule of 5, which indicates that these compounds present physicochemical properties suitable for herbicides.

© 2015 Elsevier B.V. All rights reserved.

### 1. Introduction

In recent decades, increasing agricultural productivity has been a necessary and challenging task. The production of food for a growing world population coupled to the allocation of cropland to biofuel production without expanding the agricultural frontier into natural ecosystems requires increasing agricultural yields *per* hectare. Therefore, the reduction of any crop losses to agricultural pests becomes a great concern.

Because weeds are one of the major pests causing agricultural losses worldwide, the maintenance of high agricultural yields is highly dependent on the chemical control of such invasive plants [1,2]. However, the continuous application of herbicides has resulted in selective pressure, leading to the replacement of sensitive biotypes by herbicide-resistant biotypes. The shift in the weed spectrum in diverse croplands has made weed management an even more difficult task [3–5]. Compounding this situation, no herbicide with a major new mode of action has been introduced into the market in the last two decades [6]. In view of this scenario, it is imperative to discover new herbicide molecules that are capable of acting through novel mechanisms of action and additionally present benign environmental and toxicological profiles. To meet this

demand, academic and industrial studies have focused on the search for natural products as models for the development of novel herbicides [7–9].

In line with this tendency, our research group has synthesized and investigated the phytotoxic activity of a range of analogues to naturally occurring  $\gamma$ -alkylidene butenolides [10–16]. In a recent work, we found that synthetic analogues of rubrolides, namely a class of natural butenolides, were almost as effective as the commercial herbicide DCMU in inhibiting the photosynthetic electron transport chain [10]. In the same study [10], a quantitative structure–activity relationship (QSAR) analysis showed that the photosynthesis-inhibitory activity of these compounds is strongly related to their ability to accept electrons and with their polarity.

Through cyclic voltammetry and computational methods, we found that the ability of a series of rubrolide analogues to interfere with the Hill reaction is closely related to their redox potential: an inhibitor with a higher first-reduction potential is associated with increased effectiveness [11].

In this manuscript, we report a more comprehensive study that was performed to obtain in-depth insights on how different substitution patterns on the rubrolide analogues may influence their photosynthesis-inhibitory properties. The range of compounds tested includes both previously synthesized molecules [11] and novel analogues, the synthesis and characterization of which are also reported in this manuscript.

With the aim of obtaining a better understanding of their mode of action, the effects of the rubrolide analogues on various

\* Corresponding author at: Department of Chemistry, Universidade Federal de Minas Gerais, Av. Pres. Antônio Carlos, 6627, Campus Pampulha, CEP 31270-901 Belo Horizonte, MG, Brazil. Tel.: +55 31 34093396.

E-mail addresses: [lcab@ufmg.br](mailto:lcab@ufmg.br), [lcab@outlook.com](mailto:lcab@outlook.com) (L.C.A. Barbosa).

photosynthetic processes, including the electron transport rate (basal, phosphorylating and uncoupled), partial reactions of PSI and PSII and the chlorophyll *a* fluorescence transients, were measured. The influence of the structural diversity of the rubrolide analogues on their ability to interfere with these different photosynthetic processes are discussed in the manuscript.

## 2. Materials and methods

### 2.1. General experimental

All of the reagents and solvents were prepared following procedures already reported in the literature [17] or were purchased from commercially available suppliers and used without any further purification. The reported melting points are uncorrected and were obtained using a MQAPP-301 melting point apparatus (Microquímica, Brazil). Analytical thin layer chromatography analysis was conducted on aluminum-packed pre-coated silica gel plates. Column chromatography was performed over silica gel 230–400 mesh. All of the compounds were fully characterized by IR, EI-MS, <sup>1</sup>H NMR, <sup>13</sup>C NMR, COSY, HETCOR and NOEDIFF NMR spectroscopy. The infrared spectra were recorded on a Perkin-Elmer Paragon 1000 FTIR spectrophotometer using potassium bromide (1% w/w) disks or thin liquid film on NaCl plates. The mass spectra were recorded on a Shimadzu GCMS-QP5050A instrument by direct insertion using the EI mode (70 eV). The <sup>1</sup>H NMR and <sup>13</sup>C NMR spectra were recorded on a Varian Mercury 300 spectrometer at 300 and 75 MHz, respectively, using CDCl<sub>3</sub> or (CD<sub>3</sub>)<sub>2</sub>CO as solvents and TMS as an internal reference, unless otherwise stated. Compounds **2–29** were obtained by employing a synthetic procedure previously described [10,11]. The spectroscopic assignments for compounds **2** and **9–29** agreed with those reported in the literature [11,18]. The structures of compounds **3–8** are supported by the spectroscopic data reported below.

(*Z*)-3-Bromo-5-(3-methoxybenzylidene)-4-phenylfuran-2(5*H*)-one, **3**. The compound was a yellow solid obtained at 70% yield. Melting point (mp) 106.5–107.4 °C. FT-IR (KBr)  $\bar{\nu}_{\max}$  cm<sup>-1</sup> 3013, 2960, 2933, 2833, 1773, 1571, 1478, 1447, 1290, 1254, 1161, 1049, 981, 874, 770, 745, 686. <sup>1</sup>H NMR  $\delta_{\text{H}}$  (300 MHz, CDCl<sub>3</sub>) 3.84 (s, 3H), 6.11 (s, 1H), 6.90–6.94 (m, 1H), 7.26–7.36 (m, 4H), 7.51–7.59 (m, 4H). <sup>13</sup>C NMR  $\delta_{\text{C}}$  (75 MHz, CDCl<sub>3</sub>) 55.7, 109.1, 114.9, 115.8, 116.3, 124.0, 129.3, 129.4, 130.2, 130.9, 134.1, 148.0, 154.2, 160.1, 165.3. MS, *m/z* (%) 358 (M<sup>+</sup>+2, 52), 356 (M<sup>+</sup>, C<sub>18</sub>H<sub>13</sub>BrO<sub>2</sub>, 52), 277 (31), 249 (31), 221 (100), 178 (25), 148 (36), 129 (47), 125 (20), 91 (37), 89 (21), 77 (25), 51 (50).

(*Z*)-3-Bromo-5-(4-fluorobenzylidene)-4-phenylfuran-2(5*H*)-one, **4**. The compound was obtained as a yellow solid at 44% yield. Melting point (mp) 138.8–139.3 °C. FT-IR (KBr)  $\bar{\nu}_{\max}$  cm<sup>-1</sup> 3061, 1771, 1600, 1508, 1239, 1163, 955, 830, 748, 697. <sup>1</sup>H NMR  $\delta_{\text{H}}$  (300 MHz, CDCl<sub>3</sub>) 6.10 (s, 1H), 7.08 (t, 2H, *J* = 8.7 Hz), 7.50–7.59 (m, 5H), 7.78 (dd, 2H, *J* = 5.4 Hz, *J* = 8.7 Hz). <sup>13</sup>C NMR  $\delta_{\text{C}}$  (75 MHz, CDCl<sub>3</sub>) 108.5, 113.3, 116.1 (d, *J* = 21.8 Hz), 128.8, 128.8 (d, *J* = 2.3 Hz), 128.9, 130.0, 130.5, 132.8 (d, *J* = 8.3 Hz), 147.1, 153.8, 163.2 (*J* = 255 Hz), 164.9. MS, *m/z* (%) 346 (M<sup>+</sup>+2, 35), 344 (M<sup>+</sup>, C<sub>17</sub>H<sub>10</sub>BrFO<sub>2</sub>, 36), 209 (100), 136 (39), 129 (40), 108 (66), 107 (31), 75 (23).

(*Z*)-3,4-Dibromo-5-(4-fluorobenzylidene)furan-2(5*H*)-one, **5**. The compound was obtained as a yellow solid at 14% yield. Melting point (mp) 178.5–180.0 °C. FT-IR (KBr)  $\bar{\nu}_{\max}$  cm<sup>-1</sup> 3059, 1767, 1603, 1547, 1511, 1247, 1166, 992, 966, 826. <sup>1</sup>H NMR  $\delta_{\text{H}}$  (300 MHz, CDCl<sub>3</sub>) 6.41 (s, 1H), 7.11 (t, 2H, *J* = 8.7 Hz), 7.81 (dd, 2H, *J* = 5.4 Hz, *J* = 8.7 Hz). <sup>13</sup>C NMR  $\delta_{\text{C}}$  (75 MHz, CDCl<sub>3</sub>) 112.9, 113.0, 116.3 (d, *J* = 21.8 Hz), 128.1 (d, *J* = 3.8 Hz), 133.1 (d, *J* = 8.3 Hz), 137.4, 145.2, 163.3, 163.5 (*J* = 252 Hz). MS, *m/z* (%) 350 (M<sup>+</sup>+4, 36), 348 (M<sup>+</sup>+2, 74), 346 (M<sup>+</sup>, C<sub>11</sub>H<sub>5</sub>Br<sub>2</sub>FO<sub>2</sub>, 36), 213

(47), 211 (48), 136 (54), 133 (22), 132 (22), 131 (35), 108 (100), 107 (74), 57 (26).

(*Z*)-3,4-Dibromo-5-(4-(trifluoromethyl)benzylidene)furan-2(5*H*)-one, **6**. The compound was obtained as a yellow solid at 31% yield. Melting point (mp) 137.0–137.8 °C. FT-IR (KBr)  $\bar{\nu}_{\max}$  cm<sup>-1</sup> 3073, 1792, 1614, 1551, 1417, 1323, 1186, 1181, 1107, 1163, 980, 875. <sup>1</sup>H NMR  $\delta_{\text{H}}$  (300 MHz, CDCl<sub>3</sub>) 6.46 (s, 1H), 7.25 (d, 2H, *J* = 8.4 Hz), 7.73 (d, 2H, *J* = 8.4 Hz). <sup>13</sup>C NMR  $\delta_{\text{C}}$  (75 MHz, CDCl<sub>3</sub>) 112.0, 114.5, 125.9 (q, *J* = 3.8 Hz), 128.5 (q, *J* = 267.8 Hz), 130.9, 131.0 (q, *J* = 32.3 Hz), 135.7, 137.4, 146.9, 162.8. MS, *m/z* (%) 400 (M<sup>+</sup>+4, 46), 398 (M<sup>+</sup>+2, 100), 396 (M<sup>+</sup>, C<sub>12</sub>H<sub>5</sub>Br<sub>2</sub>F<sub>3</sub>O<sub>2</sub>, 48), 263 (53), 261 (60), 186 (70), 158 (82), 133 (27), 131 (32), 89 (23), 86 (22), 84 (31), 63 (26), 51 (25).

(*Z*)-3,4-Dibromo-5-(4-ethylbenzylidene)furan-2(5*H*)-one, **7**. The compound was obtained as a yellow solid at 47% yield. Melting point (mp) 104.7–105.8 °C. FT-IR (KBr)  $\bar{\nu}_{\max}$  cm<sup>-1</sup> 3041, 2964, 2929, 2871, 1782, 1601, 1205, 846, 739, 621. <sup>1</sup>H NMR  $\delta_{\text{H}}$  (300 MHz, CDCl<sub>3</sub>) 1.26 (t, 2H, *J* = 7.5 Hz), 2.68 (q, 3H, *J* = 7.5 Hz), 6.43 (s, 1H), 7.25 (d, 2H, *J* = 8.4 Hz), 7.80 (d, 2H, *J* = 8.4 Hz). <sup>13</sup>C NMR  $\delta_{\text{C}}$  (75 MHz, CDCl<sub>3</sub>) 15.2, 28.9, 112.4, 114.5, 128.6, 129.3, 131.1, 137.4, 145.0, 147.1, 163.5. MS, *m/z* (%) 360 (M<sup>+</sup>+4, 19), 358 (M<sup>+</sup>+2, 39), 356 (M<sup>+</sup>, C<sub>13</sub>H<sub>10</sub>Br<sub>2</sub>O<sub>2</sub>, 19), 345 (20), 343 (35), 341 (23), 131 (100), 117 (21), 115 (29), 77 (41), 63 (26), 51 (24), 39 (30).

(*Z*)-3,4-Dibromo-5-(3-methoxybenzylidene)furan-2(5*H*)-one, **8**. The compound was obtained as a yellow solid at 67% yield. Melting point (mp) 151.0–151.6 °C. FT-IR (KBr)  $\bar{\nu}_{\max}$  cm<sup>-1</sup> 3063, 3044, 3015, 2967, 2941, 2839, 1765, 1649, 1596, 1549, 1307, 1237, 1191, 1040, 979, 880, 789, 684, 637. <sup>1</sup>H NMR  $\delta_{\text{H}}$  (300 MHz, CDCl<sub>3</sub>) 3.85 (s, 3H), 6.41 (s, 1H), 6.96 (ddd, 3H, *J* = 7.8 Hz, *J* = 2.7 Hz, *J* = 1.5 Hz), 6.97–7.39 (m, 3H). <sup>13</sup>C NMR  $\delta_{\text{C}}$  (75 MHz, CDCl<sub>3</sub>) 55.4, 113.2, 114.1, 115.6, 116.4, 123.8, 130.1, 133.0, 137.5, 145.7, 159.8, 163.2. MS, *m/z* (%) 363 (M<sup>+</sup>+4, 47), 360 (M<sup>+</sup>+2, 100), 358 (M<sup>+</sup>, C<sub>12</sub>H<sub>8</sub>Br<sub>2</sub>O<sub>2</sub>, 50), 281 (37), 279 (45), 225 (53), 223 (56), 167 (24), 149 (80), 148 (57), 91 (46), 86 (31), 84 (51), 77 (38), 71 (38), 63 (23), 57 (69), 55 (39), 51 (90), 50 (30).

### 2.2. Chloroplasts isolation and chlorophyll determination

Intact chloroplasts were isolated from spinach leaves (*Spinacia oleracea* L.) obtained from a local market as previously described [19,20]. The chloroplasts were isolated with a medium that contained 400 mM sucrose, 5 mM MgCl<sub>2</sub>, and 10 mM KCl and was buffered with 3 mM K<sup>+</sup>-tricine at pH 8.0. The chloroplasts were re-suspended in the same medium and stored as a concentrated suspension in the dark at 4.0 °C while using. The chlorophyll concentration was measured spectrophotometrically as previously reported [21].

### 2.3. Measurement of non-cyclic electron transport rate

The light-induced non-cyclic electron transport activity from water to methylviologen (MV) was determined with a YSI (Yellow Springs Instrument) oxygen monitor (model 5300) using a Clark-type electrode as previously published [19,20]. The chloroplasts (equivalent of 20 µg/mL of chlorophyll) were freshly lysed in 3 mL of the basal electron transport reaction medium, which was composed of 100 mM sorbitol, 5 mM MgCl<sub>2</sub>, 10 mM KCl, 0.5 mM KCN, 30 mM K<sup>+</sup>-tricine at pH 8.0 and 50 µM MV, and the basal electron flow was measured by polarography. The phosphorylating non-cyclic electron transport from water to MV was measured with basal non-cyclic electron transport medium supplemented with 1 mM ADP and 3 mM KH<sub>2</sub>PO<sub>4</sub>. The uncoupled electron transport from water to MV was tested using the same protocol as that used for the measurement of the basal non-cyclic electron transport with the exception that 6 mM NH<sub>4</sub>Cl was added as an uncou-

pler to the medium. All of the reaction mixtures were illuminated for 2 min with a projector lamp (Gaf 2669) and passed through a 5 cm filter of a 1% CuSO<sub>4</sub> solution to result in actinic light (0.2 mW/cm<sup>2</sup>).

#### 2.4. Determination of uncoupled photosystem II (PSII) and uncoupled photosystem I (PSI) electron flow

The uncoupled PSII from water to 2,5-dichloro-1,4-benzoquinone (DCBQ) was monitored polarographically [22]. DCBQ accepts electrons at the D<sub>1</sub> protein, and thus, we measured the electron transport from water to Q<sub>B</sub>. The reaction medium for assaying PSII activity was the same as that used for basal electron transport with the exception that MV was omitted and 1 μM 2,5-dibromo-6-isopropyl-3-methyl-1,4-benzoquinone (DBMIB), 100 μM DCBQ and 6 mM NH<sub>4</sub>Cl were added. The partial reaction of PSII electron transport from water to sodium silicomolybdate (SiMo) was determined using the same protocol as that used for PSII with the same basal electron transport medium without MV and supplemented with 50 μM SiMo and 10 μM 3-(3,4-dichlorophenyl)-1,1-dimethylurea (DCMU) [23]. These electron flow activities were monitored with a YSI oxygen monitor (model5300) using a Clark-type electrode.

The uncoupled PSI electron transport from 2,6-dichlorophenylindophenol (DCPIP) reduced with ascorbate was determined using the basal electron transport medium supplemented with 10 μM DCMU (to inhibit PSII at the Q<sub>B</sub> level) [24], and 100 μM DCPIP was reduced with 300 μM ascorbate and uncoupled with 6 mM NH<sub>4</sub>Cl [25]. The *I*<sub>50</sub> value for each activity was extrapolated using the graph of the percentage of activity as a function of the compound concentration. *I*<sub>50</sub> is the concentration resulting in 50% inhibition of the activity.

#### 2.5. Chlorophyll *a* fluorescence of PSII measurements in thylakoids

The chlorophyll *a* fluorescence transients were measured with a Handy-PEA (Plant Efficient Analyzer, from Hansatech, King's Lynn, Norfolk, UK) as previously described [20]. The maximum fluorescence yield from the sample was generated by illumination for 2 s with continuous light (650 nm peak wavelength, intensity equivalent to 2830 μmol photons m<sup>-2</sup> s<sup>-1</sup> and gain of 0.7) provided by an array of three light-emitting diodes. The reaction medium used was that employed in the basal non-cyclic electron transport measurements with MV. To monitor the Chl *a* fluorescence transients, aliquots of dark-adapted thylakoids containing 60 μg of Chl were incubated for 5 min in 3 mL of the basal electron transport medium without MV and with different concentrations of the tested compounds, and the control contained medium plus the amount of DMSO employed for each compound at the different concentrations tested. The solutions were then centrifuged at 1269g for 5 min. The pellets containing the thylakoids were transferred to 1.5 cm<sup>2</sup> of filter paper by gravity with a dot-blot apparatus (Bio-Rad, United States) to ensure a homogeneous and reproducible distribution of the thylakoids. The filter paper was immediately placed in a clip, and the fluorescence was measured.

The OJIP transients were analyzed according to the JIP test, and the measured parameters were the following: fluorescence intensity level (*F*<sub>0</sub>) when the plastoquinone electron acceptor pool (Q<sub>A</sub>) is fully oxidized and fluorescence level when Q<sub>A</sub> is transiently fully reduced (*F*<sub>M</sub>). *F*<sub>1</sub> = 0.05 ms, *F*<sub>3</sub> = *F*<sub>K</sub> (or F300us); *F*<sub>4</sub> = *F*<sub>J</sub> (2 ms); *F*<sub>5</sub> = *F*<sub>I</sub> (30 ms) [26].

The chlorophyll *a* fluorescence transients normalized using the equation  $Vt = (Ft - F_0) / (F_M - F_0)$ , and the difference between the treated and control normalized transients are plotted as a function of time, an increase in intensity between 2 and 4 ms is observed in a J-band close to 2 ms indicates an increase in the Q<sub>A</sub>

concentration. The appearance of a K-band near 0.3 ms is an indication of damage in the water splitting system on thylakoids [27].

### 3. Results and discussion

#### 3.1. Synthesis

All of the compounds were prepared using the same synthetic approach previously reported [10,11,28]. Briefly, brominated lactone **1** was subjected to aldol condensation using different aromatic aldehydes, *tert*-butyldimethylsilyl trifluoromethane sulfonate (TBDMSOTf) and *N,N*-diisopropylethylamine (DIPEA) (Fig. 1), to afford the adduct, which was not isolated. Then, the addition of 1,8-diazabicyclo[5.4.0] undec-7-ene (DBU) to the reaction media led to a β-elimination and the formation of compounds **5–8** at yields ranging from 14% to 67%. For the synthesis of **3** and **4**, lactone **2** was first synthesized (66% yield) through a well-established methodology [18] utilizing a Suzuki–Miyaura cross coupling between brominated lactone **1** and phenylboronic acid. Lactone **2** was then subjected to aldol condensation with *p*-fluorobenzaldehyde and *m*-methoxybenzaldehyde. A subsequent β-elimination led to compounds **3** and **4** at yields of 44% and 70%, respectively. The synthesis of compounds **9–29** has been previously reported [11], and their substitution patterns are presented in Table 1.

#### 3.2. Effect of compounds **3–29** on electron transport from water to MV in spinach chloroplasts

To investigate their photosynthesis-inhibition properties, compounds **3–29** were assayed for their effect on non-cyclic electron transport from water to MV under basal, phosphorylation, and uncoupled conditions.

Compounds **8–10**, **13–15**, **18**, **20**, **22–24**, **26** and **28** were inactive, and were not further studied. The active compounds were listed in Table 2, which show that all were capable of inhibiting the basal, uncoupled and phosphorylating electron transfer, indicating that these compounds act as Hill reaction inhibitors. The remarkable variability in the activity of these compounds clearly indicates that the presence and position of different substituents in aromatic and lactone rings exert great influence on the ability of the resulting compounds to interfere with the photosynthetic electron flow. As a general tendency, the presence of an electron-withdrawing substituent, which improves the ability of the compound to accept electrons, and hydroxyl groups, which makes the compound more hydrosoluble, plays a pivotal role on the activities of these compounds. This tendency becomes clearer when we compared those compounds with closer structural similarities. For example, compounds **11** and **12**, **21** and **19**, **17** and **14**, and **25** and **23** shows the same pattern of substitution on the benzylidene ring but differ from each other by the presence of a fluorine atom at the *para* position in the 3-phenyl ring. The comparison of these pairs of compounds revealed that the rubrolide analogue bearing the electron-withdrawing fluorine atom showed higher activity than the corresponding analogue without this substituent. This influence is also observed for compounds **3** and **4**: compound **3**, which bears a fluorine atom in the benzylidene ring, showed markedly higher activity compared with **4**, which has an electron-donating methoxyl group on the same ring. A comparison of compounds **6**, **5**, **7** and **8** makes this tendency even more evident. These compounds differ from each other only by the substituent on the benzylidene ring. Compound **6** bears a strong electron-withdrawing trifluoromethyl and showed the highest inhibitory activity. Compound **5**, which presents a fluorine atom, exhibited greater activity in uncoupled electron flux compared with compound **7**, which

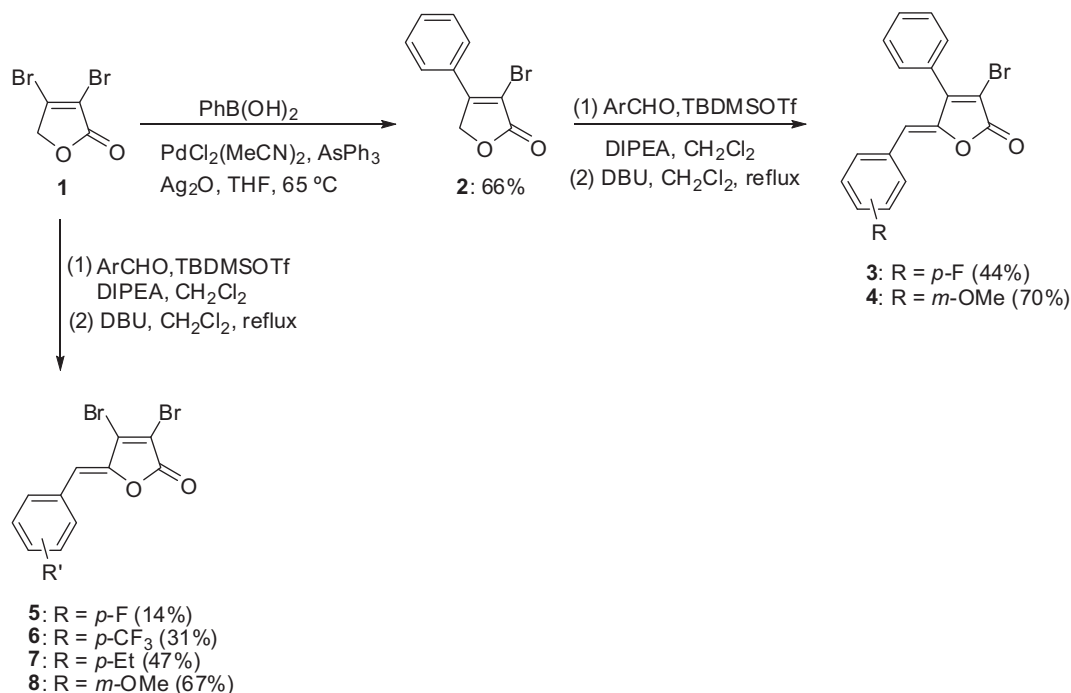


Fig. 1. Synthesis of compounds 3–8.

**Table 1**  
 Substituent groups of compounds 9–29.

Compound	R <sub>1</sub>	R <sub>2</sub>	R <sub>3</sub>	R <sub>4</sub>	R <sub>5</sub>	R <sub>6</sub>
<b>9</b>	H	OMe	H	H	Et	H
<b>10</b>	F	OMe	H	H	Et	H
<b>11</b>	H	OMe	H	H	OH	H
<b>12</b>	F	OMe	H	H	OH	H
<b>13</b>	H	OMe	OMe	H	OMe	H
<b>14</b>	H	OH	OH	H	OH	H
<b>15</b>	F	OMe	OMe	H	OMe	H
<b>16</b>	F	OMe	OH	H	OH	H
<b>17</b>	F	OH	OH	H	OH	H
<b>18</b>	H	OMe	H	OMe	OMe	H
<b>19</b>	H	OH	H	OH	OH	H
<b>20</b>	F	OMe	H	OMe	OMe	H
<b>21</b>	F	OH	H	OH	OH	H
<b>22</b>	H	OMe	OMe	H	H	OMe
<b>23</b>	H	OH	OH	H	H	OH
<b>24</b>	F	OMe	OMe	H	H	OMe
<b>25</b>	F	OH	OH	H	H	OH
<b>26</b>	H	OMe	OMe	OMe	H	H
<b>27</b>	H	OH	OH	OH	H	H
<b>28</b>	F	OMe	OMe	OMe	H	H
<b>29</b>	F	OH	OH	OH	H	H

bears an ethyl substituent. Finally, compound **8**, bearing an electron-donating methoxyl group, was found to be inactive.

In a previous study [10], we found that rubrolide analogues bearing electron-withdrawing substituents were more effective in interfering with the Hill reaction. This finding was again

observed for the new series of analogues investigated in this study, corroborating the correlation between redox potential and ability to act as a Hill reaction inhibitor [11].

The comparison of the pairs of compounds **17/15**, **19/18**, **21/20**, **25/24**, **27/26** and **29/28** revealed that the compounds presenting methoxyl groups were less active compared with those bearing hydroxyl groups. Thus, we can hypothesize that higher water solubility, which is conferred by the presence of hydroxyl groups, may influence the activity of these compounds.

This trend was also found for nostoclide analogues, another class of  $\gamma$ -alkylidenebutenolides with photosynthesis-inhibition properties: the efficacy of nostoclide as Hill reaction inhibitors was correlated with higher water solubility. As argued by the authors, higher water solubility may improve the partition between water and thylakoid membranes and consequently access to the active site [14]. It is worth mentioning that all rubrolide analogues presenting only methoxyl groups were inactive, whereas almost all hydroxylated analogues interfered with the photosynthetic electron flow (Table 2).

**Table 2**

*I*<sub>50</sub> values ( $\mu\text{M}$ ) of active compounds calculated from the basal, phosphorylating and uncoupled electron transport from water to MV in spinach thylakoids.

Compound	Basal <i>I</i> <sub>50</sub> ( $\mu\text{M}$ )	Phosphorylating <i>I</i> <sub>50</sub> ( $\mu\text{M}$ )	Uncoupled <i>I</i> <sub>50</sub> ( $\mu\text{M}$ )
<b>3</b>	4.5 ± 2.1	4.0 ± 2.2	3.3 ± 1.7
<b>4</b>	65 ± 8.6	95 ± 5.7	43 ± 6.8
<b>5</b>	35 ± 2.5	63 ± 2.8	17 ± 1.8
<b>6</b>	0.133 ± 0.04	0.339 ± 0.1	0.536 ± 0.12
<b>7</b>	22 ± 11	21 ± 9.0	26 ± 4.3
<b>11</b>	40 ± 3.5	34 ± 5.7	79 ± 6.2
<b>12</b>	33 ± 2.2	58 ± 4.5	23 ± 3.4
<b>16</b>	2.0 ± 1.2	6.2 ± 5.8	1.8 ± 0.8
<b>17</b>	2.5 ± 2.5	4.3 ± 2.0	9.7 ± 3.2
<b>19</b>	181 ± 10.5	70 ± 5.4	99 ± 14.7
<b>21</b>	91 ± 3.1	56 ± 4.6	63 ± 1.7
<b>25</b>	17 ± 7.1	14 ± 6.8	14 ± 6.2
<b>27</b>	48 ± 3.2	78 ± 4.2	63 ± 2.6
<b>29</b>	175 ± 9.6	50 ± 4.5	69 ± 3.6

**Table 3**  
Tice's parameters calculated for the active compounds.

Compound	milogP	MW	HBD	HBA	nRotb
<b>3</b>	4.747	345.167	0	2	2
<b>4</b>	4.616	357.203	0	3	3
<b>5</b>	3.741	347.965	0	2	1
<b>6</b>	4.493	397.972	0	2	2
<b>7</b>	4.512	358.029	0	2	2
<b>11</b>	4.113	373.202	1	3	4
<b>12</b>	4.252	391.192	1	3	4
<b>16</b>	4.169	407.191	2	5	3
<b>17</b>	3.893	393.164	3	5	2
<b>19</b>	3.348	375.174	3	5	2
<b>21</b>	3.487	393.164	3	5	2
<b>25</b>	3.893	393.164	3	5	2
<b>27</b>	3.553	375.174	3	5	2
<b>29</b>	3.692	393.164	3	5	2
<b>Tice<sup>29</sup></b>	≤5	150–500	≤3	2–12	≤12

Compounds **19** and **29** inhibit the phosphorylating electron transport rate to a higher degree than the basal and the uncoupled electron flow (high  $I_{50}$  values from the basal electron flux were calculated for these compounds: 181  $\mu\text{M}$  and 175  $\mu\text{M}$ , respectively). These results indicate that **19** and **29** interact more at an energized state (electron flow coupled to ATP synthesis) than in a non-energized state (basal and uncoupled electron flow) or may act by inhibiting ATP synthesis itself [29].

### 3.3. Predicted physicochemical parameters for active compounds

In a living organism, an active compound needs to cross several barriers before reaching its target site. Thus, its biological activity is greatly determined not only by its potency but also by its solubility and ability to permeate cell walls and membranes, which depends on the physicochemical properties of the compound [30,31].

“Lipinski's rule of 5” [30] is a set of empirically derived rules that delineate the physicochemical properties and molecular features of orally bioavailable drugs. Molecules violating more than one of these rules exhibited limited bioavailability [30]. This approach was modified by Tice [31] for agrochemicals. The physicochemical parameters molecular weight (MW), calculated lipophilicity (LogP), number of hydrogen-bond donors (HBD), number of hydrogen-bond acceptors (HBA), and number of rotatable bonds ( $n\text{Rotb}$ ), which is consistent with uptake and

translocation to the site of action, are encompassed by “Tice's rule” for screening new herbicide candidates [31].

To determine whether the photosynthesis-inhibitory rubrolide analogues satisfy Tice's rule, their physicochemical parameters were calculated using the Molinspiration software package [32], and these are summarized in Table 3. As observed, all of the compounds follow Tice's rule, strongly indicating that these compounds present physicochemical properties suitable for herbicides [31].

### 3.4. Localization of target sites of rubrolide analogues

To determine the target sites on the thylakoid electron transport chain, the effect of rubrolide analogues **3**, **6**, **12**, **16**, **17** and **25** on PSII, PSI, and partial reactions of photosystems were tested using artificial electron donors and acceptors, as well as appropriate inhibitors [25]. As shown in Fig. 2A and B, compounds **3**, **6**, **12**, **16**, **17** and **25** completely inhibited the uncoupled PSII electron flow from water to DCBQ, with  $I_{50}$  values of 14.5, 0.65, 3.7, 3.1, 8.3 and 2.4  $\mu\text{M}$ , respectively.

To further identify the inhibitory site of the rubrolide analogues on PSII, we measured their effects on the electron flow from water to SiMo (because SiMo accepts electrons from pheophytin, the electron flow measurements were performed from the water-splitting enzyme to pheophytin). The results indicate that the compounds did not affect this partial reaction because the rate of the treated thylakoids was similar to the control (data not shown); therefore, all of the active rubrolide analogues assayed inhibited the electron transport chain after pheophytin [23].

The uncoupled PSI electron transport rate was measured by polarography from reduced DCPIP to MV using increasing concentrations of the rubrolide analogues to determine whether they affect this photosystem. The results showed that the rates for the control and treated samples were similar. Therefore, the analogues do not interact with the PSI electron transport chain (data not shown).

The polarographic measurements suggest that compounds **3**, **6**, **12**, **16**, **17** and **25** inhibited electron transport at the acceptor side of PSII, since the rubrolide analogues have no-effect on electron transport from water to pheophytin and on electron flow of PSI.

### 3.5. Measurements of the Chl *a* fluorescence transients in thylakoids in the presence of the synthetic rubrolide analogues

To provide additional evidence of the interaction site of the rubrolide analogues at PSII, the fluorescence of chlorophyll *a* on

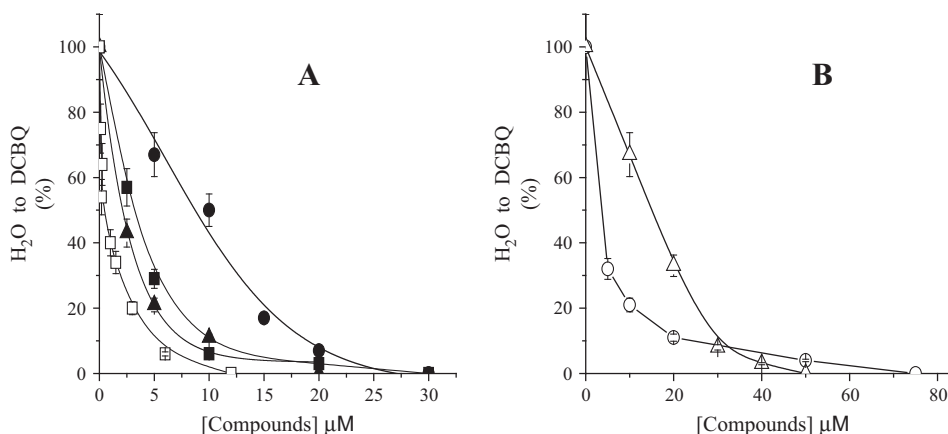


**Fig. 2.** Panel A: Effect of **6** ( $\square$ ), **16** ( $\bullet$ ), **17** ( $\blacksquare$ ) and **25** ( $\blacktriangle$ ). Panel B: Effect of **3** ( $\triangle$ ) and **12** ( $\circ$ ). The effects were measured on the uncoupled PSII electron transport from  $\text{H}_2\text{O}$  to DCBQ. The control is equal to 100% of the activity and was 311  $\mu\text{equiv e}^-/\text{mg Chl h}$ .

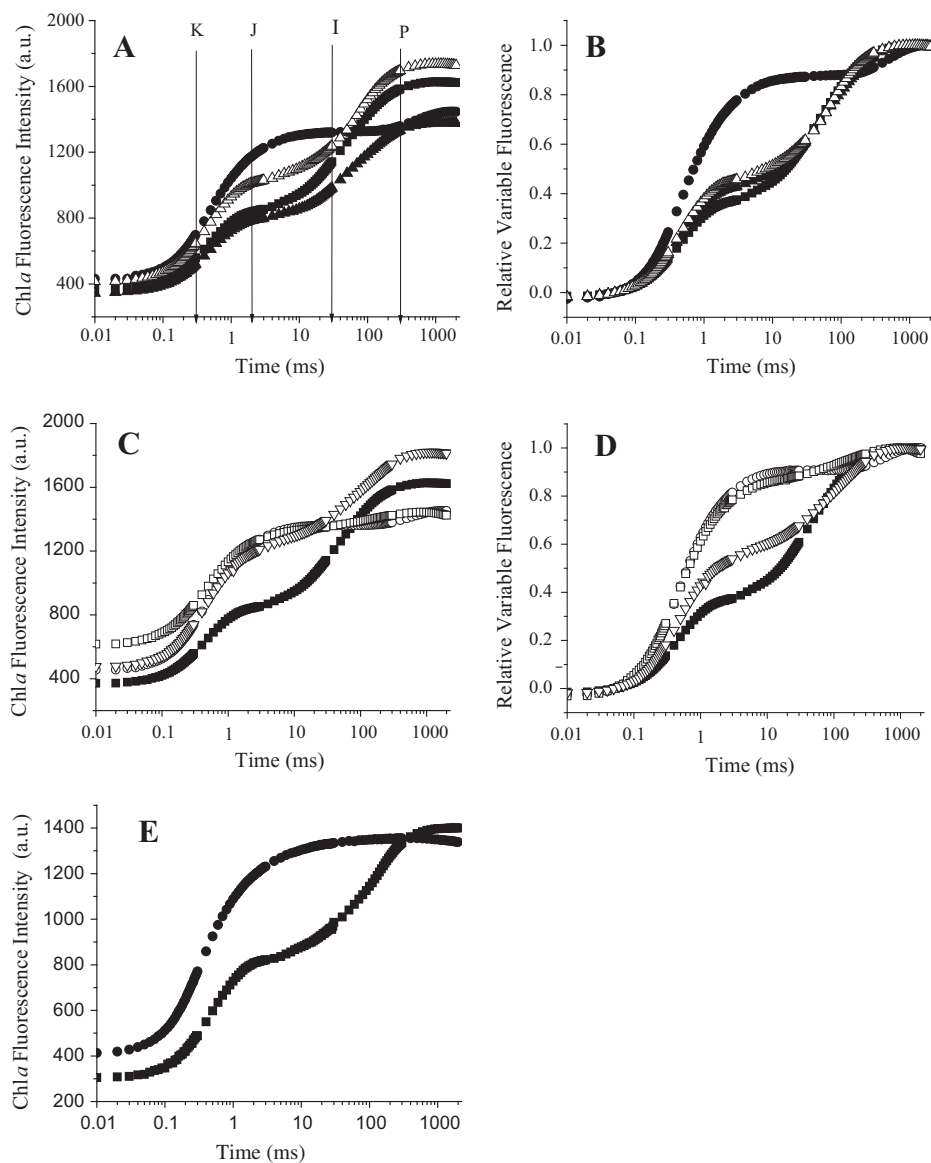


**Fig. 3.** Chl *a* fluorescence transients of the control (■) and samples treated with the following: Panel A, **3** (▲) (50  $\mu$ M), **16** (●) (30  $\mu$ M) and **25** (△) (20  $\mu$ M); Panel C, **6** (▽) (3  $\mu$ M), **12** (□) (100  $\mu$ M) and **17** (○) (30  $\mu$ M). The transients shown in Panels B and D were normalized from  $F_1$  to  $F_M$ . Panel E, Chl *a* fluorescence transients of the control (■) and samples treated with 10  $\mu$ M DCMU (●) and 0.8 M Tris (▲).

**Table 4**  
Experimental average values  $\pm$  standard deviation of chlorophyll *a* fluorescence obtained for the control and treated chloroplasts with compounds **3**, **6**, **12**, **16**, **17** and **25**. The data present the results of four replicates  $\pm$  standard deviation.

Compound ( $\mu$ M)	$F_0$	$F_M$	$F_1 = 0.050$ (ms)	$F_3 = F_K$	$F_4 = F_J$	$F_5 = F_I$	$F_M/F_0$	$F_V/F_M$
Control	354 $\pm$ 24	1627 $\pm$ 80	389 $\pm$ 24	558 $\pm$ 38	838 $\pm$ 46	1142 $\pm$ 64	4.596	0.783 $\pm$ 0.009
<b>3</b> (50)	332 $\pm$ 33	1379 $\pm$ 37	363 $\pm$ 45	520 $\pm$ 59	787 $\pm$ 12	982 $\pm$ 20	4.153	0.759 $\pm$ 0.017
<b>6</b> (3)	454 $\pm$ 33	1820 $\pm$ 34	500 $\pm$ 66	739 $\pm$ 60	1175 $\pm$ 70	1393 $\pm$ 90	4.00	0.750 $\pm$ 0.009
<b>12</b> (100)	598 $\pm$ 45	1444 $\pm$ 47	642 $\pm$ 47	859 $\pm$ 79	1236 $\pm$ 86	1351 $\pm$ 98	2.415	0.585 $\pm$ 0.039
<b>16</b> (30)	410 $\pm$ 15	1446 $\pm$ 15	456 $\pm$ 17	698 $\pm$ 29	1175 $\pm$ 30	1320 $\pm$ 18	3.527	0.716 $\pm$ 0.006
<b>17</b> (30)	430 $\pm$ 19	1452 $\pm$ 22	481 $\pm$ 26	738 $\pm$ 60	1222 $\pm$ 67	1360 $\pm$ 69	3.377	0.704 $\pm$ 0.003
<b>25</b> (20)	394 $\pm$ 46	1736 $\pm$ 51	436 $\pm$ 56	646 $\pm$ 108	1010 $\pm$ 103	1237 $\pm$ 146	4.406	0.716 $\pm$ 0.006
Control	305 $\pm$ 15	1401 $\pm$ 70	319 $\pm$ 16	488 $\pm$ 24	808 $\pm$ 40	986 $\pm$ 49	4.593	0.782 $\pm$ 0.006
DCMU (10)	413 $\pm$ 21	1355 $\pm$ 68	450 $\pm$ 22	471 $\pm$ 39	1191 $\pm$ 60	1334 $\pm$ 67	3.28	0.695 $\pm$ 0.013

freshly lysed spinach chloroplasts was measured. The control chloroplast contained the amount of DMSO used for each treatment, and the treated chloroplasts contained the compounds at the concentrations at which they were found to completely inhibit PSII through polarographic measurements. The chlorophyll *a* induction curves of the control thylakoids (Fig. 3, Panels A and B)

showed an OJIP sequence similar to that previously described for plants, green algae, and cyanobacteria [33].

The chloroplasts treated with the rubrolide analogues and the control samples showed different  $F_M$  levels (Table 4). The  $F_M$  levels of the chloroplasts treated with **16** (Fig. 3A), **17** and **12** (Fig. 2C) were decreased compared with the control; these compounds

showed the appearance of the highest J-bands. In contrast, the  $F_0$  level was increased by almost all of the compounds tested with the exception of **3**. Furthermore, the initial ( $F_0$ ) and the maximum ( $F_M$ ) values of the fluorescence rise were used to determine the quantum yield of primary photochemistry [ $\phi_{Po} = F_V/F_M = kP/(kP + kN)$ ], where  $kP$  and  $kN$  are rate constants of photochemistry and other losses of excitation energy, respectively, and  $F_V$  is the variable component of fluorescence obtained by subtraction of  $F_0$  from the  $F_M$  value [34]. The modification of the  $F_M$  and  $F_0$  levels in the presence of DCMU would imply a change in the de-excitation rate constants ( $kP$  and  $kN$ ).

The chlorophyll *a* fluorescence transients from Fig. 3A and C were normalized between  $F_1$  and  $F_M$  (Fig. 3B and D). In Fig. 3B and D it is possible to observe an increment at 2 ms, which corresponds to the J-band which is related to the accumulation of  $Q_A^-$  species, indicating that the electron transport beyond  $Q_A$  is blocked at the  $Q_B$  level similarly to that achieved with DCMU (Fig. 3E) [35]. DCMU displaces the secondary quinone acceptor,  $Q_B$ , from its binding site at the  $D_1$  protein of photosystem II (PSII) [35]. DCMU is not redox active and prevents the reoxidation of  $Q_A^-$  by forward electron transport. Since the fluorescence rise is mainly determined by the redox state of  $Q_A$  [36], blocking its re-oxidation, both the polarographic technique and the fluorescence of chlorophyll *a* indicate that the rubrolide analogues interact with and inhibit the photosynthesis system by displacing  $Q_B$ .

#### 4. Conclusions

In this study, we found that not only the presence of electron-withdrawing groups but also the hydrosolubility of rubrolide analogues exert influence on the ability of these compounds to act as photosynthesis inhibitors. These findings corroborate our previous observation that the herbicidal activity of this class of compounds is related to ability to block electron flow at the reducing side of PSII. Additionally, our results are in agreement with a previous study that showed that the ability of nostoclide analogues (another class of butenolides that is structurally similar to rubrolides) to act as photosynthesis inhibitors depends on their hydrosolubility. All of the compounds that showed ability to interfere with the basal, uncoupled and phosphorylating electron transport were investigated to determine their site of action on the thylakoid electron transport chain. Rubrolides analogues inhibit PSII by displacing  $Q_B$  at the  $D_1$  protein site, and have no effect on PSI, as demonstrated by both polarographic techniques and chlorophyll *a* fluorescence transients. Additionally, we found that all of the active rubrolide analogues follow Tice's rule of 5, which indicates that these compounds may present physicochemical properties suitable for herbicides.

#### Acknowledgments

We are grateful to the following Brazilian agencies: Conselho Nacional de Desenvolvimento Científico e Tecnológico (CNPq) and Coordenação de Aperfeiçoamento de Pessoal de Nível Superior (CAPES) for research fellowships (E.V.V.V., J.O.S.V., and L.C.A.B.) and Fundação de Amparo à Pesquisa de Minas Gerais (FAPEMIG) for supporting our research in this area. The authors also gratefully acknowledge the financial support from DGAPA-UNAM grants PAPIIT number IT102012-3 and PAIP number 4290-03 from the Faculty of Chemistry of UNAM.

#### References

- [1] E.C. Oerke, Crop losses to pests, *J. Agric. Sci.* 144 (2006) 31–43.
- [2] P. Neve, M. Vila-Aiub, F. Roux, Evolutionary-thinking in agricultural weed management, *New Phytol.* 184 (2009) 783–793.
- [3] S.B. Powles, Evolved glyphosate-resistant weeds around the world: lessons to be learnt, *Pest Manag. Sci.* 64 (2008) 360–365.
- [4] H.J. Beckie, Herbicide-resistant weed management: focus on glyphosate, *Pest Manag. Sci.* 67 (2011) 1037–1048.
- [5] S.O. Duke, S.B. Powles, Glyphosate-resistant crops and weeds: now and in the future, *AgBioForum.* 12 (2009) 346–357.
- [6] S.O. Duke, Why has no new herbicide modes of action appeared in recent years?, *Pest Manag. Sci.* 68 (2012) 502–512.
- [7] F.E. Dayan, C.L. Cantrell, S.O. Duke, Natural products in crop protection, *Bioorg. Med. Chem.* 17 (2009) 4022–4034.
- [8] C.L. Cantrell, F.E. Dayan, S.O. Duke, Natural products as sources for new pesticides, *J. Nat. Prod.* 75 (2012) 1231–1242.
- [9] R.D. Clark, A perspective on the role of quantitative structure-activity and structure-property relationships in herbicide discovery, *Pest Manag. Sci.* 68 (2012) 513–518.
- [10] L.C.A. Barbosa, A.J. Demuner, E.E.L. Borges, J. Mann, Synthesis and evaluation of the plant growth regulatory activity of 8-oxabicyclo[3.2.1] oct-6-en-3-one derivatives, *J. Braz. Chem. Soc.* 8 (1997) 19–27.
- [11] J.O.S. Varejão, L.C.A. Barbosa, C.R.A. Maltha, M.R. Lage, M. Lanznaster, J.W.M. Carneiro, G. Forlani, Voltammetric and theoretical study of the redox properties of rubrolides analogues, *Electrochim. Acta* 120 (2014) 334–343.
- [12] L.C.A. Barbosa, J.O.S. Varejão, D. Petrollino, P.F. Pinheiro, A.J. Demuner, C.R. Maltha, G. Forlani, Tailoring nostoclide structure to target the chloroplastic electron transport chain, *ARKIVOC iv* (2012) 15–32.
- [13] R.R. Teixeira, P.F. Pinheiro, L.C.A. Barbosa, J.W.M. Carneiro, G. Forlani, QSAR modeling of photosynthesis-inhibiting nostoclide derivatives, *Pest Manag. Sci.* 66 (2010) 196–202.
- [14] R.R. Teixeira, L.C.A. Barbosa, G. Forlani, D. Piló-Veloso, J.W.M. Carneiro, Synthesis of photosynthesis-inhibiting nostoclide analogues, *J. Agric. Food Chem.* 56 (2008) 2321–2329.
- [15] L.C.A. Barbosa, M.E. Rocha, R.R. Teixeira, C.R.A. Maltha, G. Forlani, Synthesis of 3-(4-bromobenzyl)-5-(arylmethylene)-5H-furan-2-ones and their activity as inhibitors of the photosynthetic electron transport chain, *J. Agric. Food Chem.* 55 (2007) 8562–8569.
- [16] L.C.A. Barbosa, A.J. Demuner, E.S. Alvarenga, A. Oliveira, B. King-Díaz, B. Lotina-Hennsen, Phyto-growth- and photosynthesis-inhibiting properties of nostoclide analogues, *Pest Manag. Sci.* 62 (2006) 214–222.
- [17] D.D. Perrin, W.L.F. Armarego, Purification of Laboratory Chemicals, fifty ed., Butterworth-Heinemann, Boston, 2003.
- [18] F. Bellina, C. Anselmi, V. Stéphane, L. Mannina, R. Rossi, Selective synthesis of (Z)-4-aryl-5-[1-(aryl)methylidene]-3-bromo-2-(5H)-furanones, *Tetrahedron* 57 (2001) 9997–10007.
- [19] J.D. Mills, P. Mitchell, P. Schurrmann, Modulation of coupling ATPase activity in intact chloroplasts, *FEBS Lett.* 191 (1980) 144–148.
- [20] T.A.M. Veiga, B. King-Díaz, A.S.F. Marques, O.M. Sampaio, P.C. Vieira, M.F.G.F. Silva, B. Lotina-Hennsen, Furoquinoline alkaloids isolated from *Balfourodendronriedelianum* as photosynthetic inhibitors in spinach chloroplasts, *J. Photochem. Photobiol., B* 120 (2013) 36–43.
- [21] H.H. Strain, T. Cope, M.A. Svec, Analytical procedures for the isolation, identification, estimation and investigation of the chlorophylls, *Methods Enzymol.* 23 (1971) 452–466.
- [22] I. Yruela, G. Montoya, P.J. Alonso, R. Picorel, Identification of the pheophytin- $Q_A$ -Fe domain of the reducing side of the photosystem II as the Cu(II)-inhibitory binding site, *J. Biol. Chem.* 266 (1991) 22847–22850.
- [23] R.T. Guaiquinta, R.A. Dilley, A partial reaction in photosystem II: reduction of silicomolybdate prior to the site of dichlorophenyl dimethyl lurea inhibition, *Biochim. Biophys. Acta* 387 (1975) 288–305.
- [24] B.R. Velthuys, Electron-dependent competition between plastoquinone and inhibitors for binding to Photosystem II, *FEBS Lett.* 126 (1981) 277–281.
- [25] J.F. Allen, N.G. Holmes, in: M.F. Hipkinns, N.R. Baker (Eds.), Photosynthesis, Energy Transduction. A Practical Approach, I.R.L. Press, Oxford, 1986, pp. 103–141.
- [26] H.-X. Jiang, L.-S. Chen, J.-G. Zheng, S. Han, N. Tang, B.R. Smith, Aluminium induced effects of photosystem II photochemistry in Citrus leaves assessed by the chlorophyll *a* fluorescence transient, *Tree Physiol.* 28 (2008) 1863–1871.
- [27] R.J. Strasser, M. Tsimilli-Michael, A. Srivastava, in: G.C. Papageorgion, Govindjee (Eds.), Chlorophyll Fluorescence: A Signature of Photosynthesis, Kluwer Academic Publishers, Netherlands, 2004, pp. 321–362.
- [28] J. Boukouvalas, L.C. McCann, Synthesis of the human aldose reductase inhibitor rubrolide L, *Tetrahedron Lett.* 51 (2010) 4636–4639.
- [29] M.L. Macías-Rubalcava, M.E.R.-V. Sobrino, C. Meléndez-González, B. King-Díaz, B. Lotina-Hennsen, Selected phytotoxins and organic extracts from endophytic fungus *Edeniagomezpompae* as light reaction of photosynthesis inhibitors, *J. Photochem. Photobiol., B* 138 (2014) 7–26.
- [30] C.A. Lipinski, F. Lombardo, B.W. Dominy, P.J. Feeney, Experimental and computational approaches to estimate solubility and permeability in drug discovery and development settings, *Adv. Drug Deliv. Rev.* 23 (1997) 3–25.
- [31] C.M. Tice, Selecting the right compounds for screening: does Lipinski's Rule of 5 for pharmaceuticals apply to agrochemicals?, *Pest Manag. Sci.* 57 (2001) 3–16.
- [32] MolinspirationCheminformatics, Bratislava, Slovak Republic, <<http://www.molinspiration.com>>.
- [33] R.J. Strasser, A. Srivastava, Govindjee, Polyphasic chlorophyll *a* fluorescence transients in plants and cyanobacteria, *Photochem. Photobiol.* 61 (1995) 32–42.

- [34] M. Kitajima, W.L. Butler, Quenching of chlorophyll fluorescence and primary photochemistry in chloroplasts by dibromothymoquinone, *Biochim. Biophys. Acta* 376 (1975) 105–115.
- [35] S.Z. Tóth, G. Schansker, R.J. Strasser, In intact leaves, the maximum fluorescence level (FM) is independent of the redox state of the plastoquinone pool: A DCMU-inhibition study, *Biochim. Biophys. Acta* 1708 (2005) 275–282.
- [36] L.N.M. Duysens, H.E. Sweers, Mechanisms of two photochemical reactions in algae as studied by means of fluorescence, studies on microalgae and photosynthetic bacteria. Special Issue of Plant and Cell Physiology, Japanese Society of Plant Physiologists, University of Tokyo Press, considerable simplification of the Tokyo, Japan, 1963, pp. 353–372.